Cavendish-HEP-14/09
PSI-PR-14-10
SLAC-PUB-16077
TTK-14-20
DAMTP-2014-54

Improved cross-section predictions for heavy charged Higgs boson production at the LHC

Martin Flechl[1,2], Richard Klees[3], Michael Krämer[3,4], Michael Spira[5], and Maria Ubiali[6,7]

[1] *Physikalisches Institut, Freiburg University, Hermann-Herder Str. 3a, D-79104 Freiburg, Germany*
[2] *Institute of High Energy Physics, Austrian Academy of Sciences, Nikolsdorfergasse 18, A-1050 Vienna, Austria*
[3] *Institute for Theoretical Particle Physics and Cosmology, RWTH Aachen University, D-52056 Aachen, Germany*
[4] *SLAC National Accelerator Laboratory, Stanford University, Stanford, CA 94025, USA*
[5] *Paul Scherrer Institut, CH-5232 Villigen PSI, Switzerland*
[6] *Cavendish Laboratory, University of Cambridge, J.J. Thomson Avenue, CB3 0HE, Cambridge, UK*
[7] *Department of Applied Mathematics and Theoretical Physics, University of Cambridge, Wilberforce Road, CB3 0WA, Cambridge, UK*

Abstract:

In most extensions of the Standard Model, heavy charged Higgs bosons at the LHC are dominantly produced in association with heavy quarks. An up-to-date determination of the next-to-leading order total cross section in a type-II two-Higgs-doublet model is presented, including a thorough estimate of the theoretical uncertainties due to missing higher-order corrections, parton distribution functions and physical input parameters. Predictions in the four- and five-flavour schemes are compared and reconciled through a recently proposed scale-setting prescription. A four- and five-flavour scheme matched prediction is provided for the interpretation of current and future experimental searches for heavy charged Higgs bosons at the LHC.

1 Introduction

Many extensions of the Standard Model (SM), in particular supersymmetric theories, require two Higgs doublets, leading to five physical scalar Higgs bosons, including two (mass-degenerate) charged particles $H^{\pm}$. Imposing natural flavour conservation, there are four different ways to couple the SM fermions to two Higgs doublets. Each of these four ways of assigning the couplings gives rise to a different phenomenology for the charged Higgs boson. Here the focus is on a type-II two-Higgs-doublet model (2HDM), in which one doublet generates the masses of the up-type quarks and the other of down-type quarks and charged leptons.

Searches at LEP have set a limit $m_{H^{\pm}} > 80\,\text{GeV}$ on the mass of a charged Higgs boson for this model [1]. For a branching ratio $\text{BR}(H^{\pm} \to \tau\nu) = 1$, corresponding to the limit of large $\tan\beta$, the lower limit is 94 GeV [1]. The Tevatron experiments place upper limits on $\text{BR}(t \to bH^{+})$ in the $(15-20)\%$ range for $m_{\text{H}^{+}} < m_t$ [2, 3] which have recently been superseded by results of the LHC experiments: preliminary ATLAS results [4] for a type-II 2HDM exclude $\text{BR}(t \to bH^{+})$ larger than $(0.24-2.1)\%$ for $90\,\text{GeV} < m_{H^{\pm}} < 160\,\text{GeV}$ and for the first time also provide cross-section limits on $tH^{\pm}$ production in the mass range $180\,\text{GeV} < m_{H^{\pm}} < 600\,\text{GeV}$, both with the assumption that $\text{BR}(H^{\pm} \to \tau\nu) = 1$. Based on the same assumptions, CMS results [5] exclude $\text{BR}(t \to bH^{+})$ above $(2-4)\%$ for charged Higgs boson masses between 80 and 160 GeV. The search for a charged Higgs boson is a central part of the physics program at the Large Hadron Collider (LHC), and a discovery would provide unambiguous evidence for an extended Higgs sector beyond the SM.

In this paper the focus is on heavy charged Higgs bosons, $m_{H^{\pm}} > m_t$. Their main production mechanism at the LHC in most extensions of the SM proceeds through associated production with a top quark,

$$pp \to tH^{\pm}(b) + X. \tag{1}$$

In a two-Higgs doublet model of type II, like the minimal supersymmetric extension of the SM, the Yukawa coupling of the charged Higgs boson H^{-} to a top quark and bottom antiquark is given by

$$g_{t\bar{b}H^{-}} = \sqrt{2}\left(\frac{m_t}{v}P_R \cot\beta + \frac{m_b}{v}P_L \tan\beta\right), \tag{2}$$

where $v = \sqrt{v_1^2 + v_2^2} = (\sqrt{2}G_F)^{-\frac{1}{2}}$ is the Higgs vacuum expectation value in the SM, with the Fermi constant $G_F = 1.16637 \times 10^{-5}\ \text{GeV}^{-2}$ [6]. The parameter $\tan\beta = v_2/v_1$ is the ratio of the vacuum expectation values v_1 and v_2 of the two Higgs doublets, and $P_{R/L} = (1 \pm \gamma_5)/2$ are the chirality projectors.

There exist two ways of calculating the associated production of charged Higgs bosons with a top quark and an untagged bottom quark. One option, which is straightforward from the conceptual point of view, is to consider the bottom quark mass to be of the same order of magnitude as the other hard scales involved in the process. Then, the bottom quark does not contribute to the proton wave function and can only be generated as a massive final state. In practice, the theory which is used in such a calculation is an effective theory with four light quarks, where the bottom quarks are decoupled and do not enter the computation of the running coupling constant and the evolution of the parton distribution functions (PDFs). According to this approach, named four-flavour

(4F) scheme, the lowest-order QCD production processes are gluon-gluon fusion and quark-antiquark annihilation, $gg \to tbH^{\pm}$ and $q\bar{q} \to tbH^{\pm}$, respectively. The former is dominant at the LHC due to the large gluon-gluon luminosity. In the 4F scheme, computations are more involved due to the higher final-state multiplicity and because the additional final state particle is massive. However, the kinematics of the heavy quark is correctly taken into account already at the leading order, and the interface with parton shower codes is straightforward. The drawback is that potentially large logarithms of the ratio of the hard scale of the process and the mass of the bottom quark, which arise from the splitting of incoming gluons into nearly collinear $b\bar{b}$ pairs, are not summed to all orders in perturbation theory.

Such a summation is achieved in the so-called five-flavour (5F) scheme, in which the bottom quark mass is considered to be much smaller than the other scales involved in the process and consequently is ignored. The bottom quarks are treated as massless partons which are constituents of the proton and may thus appear in the initial state. Using bottom quark PDFs requires the approximation that, at leading order, the outgoing b quark has small transverse momentum and is massless, and that the virtual b quark is quasi on-shell. In this scheme, the logarithms associated to the initial state collinear splitting are resummed to all orders in perturbation theory by means of the DGLAP evolution of the bottom parton densities [7, 8]. The leading-order (LO) process for the inclusive $tH^{\pm}$ cross section is gluon-bottom fusion, $gb \to tH^{\pm}$. The next-to-leading order (NLO) cross section in the 5F scheme comprises $\mathcal{O}(\alpha_s)$ corrections to $gb \to tH^{\pm}$, including the LO contributions of the 4F calculation, $gg \to tbH^{\pm}$ and $\bar{q}q \to tbH^{\pm}$. The $m_b = 0$ approximation in the 5F scheme can be systematically improved by introducing $m_b \neq 0$ in higher-order contributions corresponding to diagrams where the b quark only appears in the final state (see for example Reference [9] and references therein).

To all orders in perturbation theory the improved 5F scheme and the 4F scheme are identical, but the way of ordering the perturbative expansion is different and at a finite order the results do not match exactly. For some processes the difference between calculations performed in the two schemes was found to be very significant at leading order. One of the most striking examples is the discrepancy which was initially observed in inclusive neutral Higgs boson production initiated by b quarks, see Reference [10]. In the leading-order analysis, setting the renormalisation and factorisation scales to $\mu_f = m_H$, the 5F scheme prediction exceeds the 4F scheme prediction by more than a factor of five. This has led to several thorough studies aiming to shed light on the origin of this difference [8,11–14]. It has been shown that a choice such as $\mu_f = m_H/4$ leads to a reduced scale dependence in both approaches and that the discrepancy between the schemes was reduced [15, 16], thus suggesting that the scale at which the gluon splits is softer than the scale of the hard process where the Higgs boson is produced. With this scale choice, the four- and five-flavour scheme calculations numerically agree within their respective uncertainties once higher-order QCD corrections are taken into account.

A recent analysis presented in Reference [17] investigates the dynamical origin of such a scale choice for generic processes involving bottom quarks in the initial state at the LHC. It is shown, contrary to naïve expectations, that unless the mass of the produced particles is very large, the effect of initial-state collinear logarithms involving the effective scale $\mathcal{Q}$ and the bottom quark mass, $\log(\mathcal{Q}^2/m_b^2)$, is always modest. Even though total cross sections computed in the 5F scheme exhibit a smaller scale uncertainty, such initial

state collinear logarithms do not spoil the convergence of perturbation theory in 4F scheme calculations. One of the reasons of this perturbative behaviour is that the effective scale $\mathcal{Q}$ which enters the initial-state collinear logarithms is significantly smaller than the hardest scale in the process. The effective scale is modified by universal phase-space factors that tend to reduce the size of the logarithms for processes taking place at hadron colliders. This provides a simple rule to choose the factorisation scale at which to perform comparisons between calculations in the 4F and 5F schemes. The scale turns out to be similar to the previous choice of $\mu_f = m_{H^\pm}/4$ for the bottom quark PDF in the 5F scheme, based on considerations on the transverse momentum of the bottom quark [18].

If the charged Higgs boson is discovered at a high mass, $m_{H^\pm} \gg m_t$, then it will be instructive to assess the impact of the resummation of the collinear logs $(m_{H^\pm}/m_t)$ into top-quark PDFs and comparing the 5F to the 6F scheme in one of the possible scenarios of a future 100 TeV collider, see e.g. Reference [19].

Next-to-leading order predictions for heavy charged Higgs boson production at the LHC in a type-II two-Higgs-doublet model have been made in the past in both 5F [18, 20–24] and 4F schemes [12, 25], including also electroweak corrections [26, 27]. In the work presented here, the NLO-QCD predictions are updated and improved by adopting the new scale setting procedure [17] mentioned above. A thorough account of all sources of theoretical uncertainties is given, state-of-the-art PDF sets are used and uncertainties are consistently combined. A matched prediction [28] for the four- and five-flavour scheme calculations is provided. Furthermore, results for a large range of $\tan\beta$ are presented which allows the comparison between theory and experiment for a wide class of beyond-the-SM scenarios. This work has been performed within the LHC Higgs Cross Section Working Group [29], and first preliminary results have been presented in Reference [30].

2 Theoretical Settings

In Sections 3 and 4, the total cross sections for associated top quark and charged Higgs boson production are calculated using the five- and the four-flavour schemes, respectively. In this section the generic settings of the two calculations are specified, and the method of estimating the theoretical uncertainty is presented.

All cross sections are computed for a type-II 2HDM, for which the coupling between a charged Higgs boson, a bottom antiquark and a top quark is given in Equation (2).[1] The only parameters that enter the calculation are thus the particle masses and $\tan\beta$, so that the results are rather generic. However, for supersymmetric models, additional higher-order contributions through the virtual exchange of supersymmetric particles need to be included. Of particular relevance are corrections that modify the tree-level relation between the bottom quark mass and its Yukawa coupling. These corrections are enhanced at large $\tan\beta$ and can be summed to all orders through a modification of the Yukawa coupling, see References [12, 31–39]. The remaining SUSY-QCD effects are marginal at large $\tan\beta$, but can reach up to O(10%) at small $\tan\beta$. Specifically, for the benchmark point SPS1b [40] the SUSY-QCD effects beyond those contained in the Yukawa coupling amount to $-(6/8/5/0.1)\%$ for $\tan\beta = 3/5/10/30$, respectively.

[1] Charged Higgs boson production in a type-I 2HDM is discussed in Section 6.

Note that throughout this paper results are given for the tH^- final state. The charge conjugate final state $\bar{t}H^+$ can be included by multiplying the results presented here by a factor of two.

There are two different sources of theoretical uncertainties that need to be taken into account: scale uncertainties which should reflect the error due to the omission of corrections beyond NLO, and parametric uncertainties induced by the error on the input parameters.

The scales that enter the calculation of heavy charged Higgs boson production comprise the renormalisation scale μ_r which determines the running of α_s, the factorisation scale μ_f which determines the evolution of the parton distribution functions, and the scale μ_b which determines the running bottom quark mass in the Yukawa coupling. To estimate the overall scale uncertainty, all three scales are independently varied by a factor of two about their central value, as specified in Sections 3 and 4 for the 5F and 4F schemes, respectively. To avoid spurious large logarithms, scale choices where the ratio of any of the three scales exceeds a factor of two are not taken into account. The envelope of the predictions is used to determine the overall scale uncertainty.

The input parameters relevant for heavy charged Higgs boson production are the parton distributions functions, the strong coupling α_s and the bottom quark mass m_b. The impact of the top-quark mass uncertainty on the results is negligible and thus not considered. These uncertainties are correlated as the PDF fits are performed for specific values of α_s and m_b, so care has to be taken to estimate the input parameter uncertainties in a consistent way. The computer codes employed to calculate the next-to-leading order total cross section in the two schemes have been interfaced to the LHAPDF library [41]. This made it possible to use state-of-the-art PDF sets and consistent $\alpha_s(M_Z)$ values in the PDFs and in the matrix element computation. In this analysis the charged Higgs boson cross sections are determined by using three of the most recent PDF sets, determined from global analyses of DIS and hadron collider data, namely CT10 [42], MSTW2008 [43] and NNPDF2.3 [44]. The latter set already includes the constraints coming from the early LHC data. The default General-Mass Variable Flavour Number (GM-VFN) sets are used for the computation of the 5F scheme cross section[2], while the Fixed Flavour Number (FFN) sets with $n_f = 4$ are used in the computation of the 4F cross sections. In the GM-VFN scheme a parton distribution function is associated to all partons, including the bottom quarks, above production threshold. The mass of the heavy quarks is taken into account in the DIS partonic cross sections. The GM-VFN scheme is designed to interpolate between the FFN scheme, which gives a correct description of the threshold region, and the resummation of the large collinear logarithms at large Q^2. Each PDF set adopts a variant of the GM-VFN scheme, which differs by higher-order terms associated to the matching condition. In particular, CT10 adopts a variant of the ACOT scheme [45] called ACOT-χ [9]. The Thorne-Roberts [46] VFN scheme or TR' [47] in its latest version, which emphasizes the correct threshold behaviour and includes certain higher-order terms, is adopted in the MSTW2008 PDF determination. The FONLL approach, introduced in Reference [48] in the context of hadro-production of heavy quarks and more recently applied to deep-

[2]Both CT10 and MSTW2005 evolve α_s with $n_f = 5$ at all scales, while NNPDF2.3 evolves α_s with $n_f = 6$ above the top threshold. For this computation it has been checked that freezing $n_f = 5$ above the top threshold in the predictions obtained with NNPDF2.3 does not affect the result.

inelastic structure functions [49], considers both massless and massive scheme calculations as power expansions in the strong coupling constant, and replaces the coefficient of the expansion in the former with their exact massive counterparts. The FONLL approach is adopted in the NNPDF fits.

In addition to the default GM-VFNS PDF sets, each collaboration provides a FFN scheme set with $n_f = 4$ [50, 51], which allows for a theoretically consistent cross-section prediction in a 4F scheme calculation. Other PDF fitting collaborations [52] provide as default FFNS parton sets with $n_f = 3, 4, 5$.

When the corresponding PDF set is available, a common value of α_s is chosen for the predictions according to the recent PDG average [6]: $\alpha_s(M_Z) = 0.1183 \pm 0.0012$. The PDF+$\alpha_s$ uncertainty is estimated by using the sets determined at different values of $\alpha_s(M_Z)$ provided by each collaboration, and by combining the PDF and the α_s uncertainties according to the standard prescription, as illustrated for example in Section 3.2 of Reference [53].

The pole mass of the top and bottom quarks are set to $m_t = 172.5\,\text{GeV}$ and $m_b = 4.75\,\text{GeV}$, respectively. The choice of the bottom quark mass and the corresponding uncertainty deserve careful consideration. The calculation of hadronic cross sections always involves PDFs which have an intrinsic dependence on the mass of the bottom quark. The central value for the bottom pole mass adopted here is consistent with most PDF fits, and corresponds to a $\overline{\text{MS}}$ mass of $m_b(m_b) = 4.21\,\text{GeV}$, using the two-loop QCD relation [54]. This value is close but not identical to the current PDG value, $m_b(m_b) = 4.18\,\text{GeV}$ [6], and to the recommendation from the LHC-HXSWG, $m_b(m_b) = 4.16\,\text{GeV}$. The uncertainty due to m_b, in particular the dependence of the PDFs on the bottom quark mass, is investigated by using input sets of PDFs with m_b varied by 60 MeV about its central pole mass value. As shown in Reference [50] and in the recent study of bottom quark-initiated neutral Higgs boson production [55], the bottom quark PDF exhibits a strong dependence on the bottom quark mass adopted in the PDF fit. Thus a significant dependence of the 5F scheme predictions on m_b through the bottom-quark PDF is expected. In addition, the cross section for charged Higgs boson production depends on the bottom quark mass through the bottom quark Yukawa coupling and, for the 4F scheme calculation, through the explicit m_b-dependence in the matrix element. All these uncertainties have been included in this calculation. Note that the bottom quark mass dependence of the 4F PDFs is small as m_b enters only indirectly through the DIS cross section in the global fit. However, the matrix element in the 4F scheme calculation contains a m_b-dependent collinear logarithm, which corresponds to the bottom quark PDF in the 5F scheme.

In summary, the total theoretical uncertainty quoted here includes: the PDF uncertainty δ_{PDF}, the α_s and m_b uncertainties ($\delta\alpha_s$ and δm_b), and the uncertainty due to missing higher orders in the partonic cross section, $\Delta^{\pm}_{\mu}$, estimated according to the usual procedure by varying the three different scales μ_r, μ_f and μ_b by a factor of two about their central values, as described above.

To combine the various sources of theoretical uncertainty the prescription of the LHC-HXSWG is used. The combined PDF+$\alpha_s + m_b$ uncertainty for each different PDF input set is computed first.[3] For each PDF set i the three sources of uncertainty are combined

[3] Unfortunately, not all PDF sets allow to vary α_s or m_b, as specified in the following sections. Therefore the total PDF uncertainty may be slightly underestimated.

in quadrature [53]:

$$\delta^i_{\mathrm{PDF}+\alpha_s+m_b} = \sqrt{(\delta^i_{\mathrm{PDF}})^2 + (\delta^i\alpha_s)^2 + (\delta^i m_b)^2}. \tag{3}$$

At this point, the envelope of the three predictions is used to give an estimate of the combined PDF and parametrical uncertainty $\delta_{\mathrm{PDF}+\alpha_s+m_b}$. Following Reference [53] the central prediction is defined as the midpoint of the envelope, such that the PDF+α_s + m_b uncertainty is symmetric by construction. The scale uncertainty, estimated for the central choice of input parameters, is then added linearly to the combined PDF+$\alpha_s + m_b$ uncertainty [56]:

$$\Delta^{\pm}_{\mathrm{tot}} = \pm\delta_{\mathrm{PDF}+\alpha_s+m_b} \pm \Delta^{\pm}_{\mu}\,. \tag{4}$$

Note that the scale uncertainty does not significantly depend on the choice of PDFs, and is computed by using the central `CT10` set.

Cross sections are calculated for Higgs boson masses $m_{H^\pm}$ in the range from 200 GeV to 600 GeV in steps of 20 GeV. Detailed results for $m_{H^\pm} = 200, 400$ and 600 GeV are collected in Tables 2–4. The value of $\tan\beta$ is set to 30, in correspondence to the region favoured by recent MSSM fits [57]. In Section 6 the cross section as a function of $\tan\beta$ is presented.

3 Five-flavour scheme results

In the 5F scheme, bottom quarks are treated as massless partons which appear in the initial state. The leading-order (LO) process for the inclusive $tH^\pm$ cross section is gluon-bottom fusion, $gb \to tH^\pm$. The next-to-leading order (NLO) QCD cross section in the 5F scheme has been calculated in References [18, 20–24]. All numbers presented here have been computed by interfacing the public code Prospino [58, 59] with the LHAPDF library [41].

The renormalisation scale is set to the average final state mass $\mu_r = (m_{H^\pm} + m_t)/2$. As previously discussed, the factorisation scale is set according to the method proposed in Reference [17]. There, a simple analytic formula is provided which enables a quantitative assessment of the size of the collinear logarithms resummed in a 5F computation. Hence, a factorisation scale can be chosen to optimally perform comparisons between calculations in the 4F and 5F schemes. For processes at the LHC this scale is typically smaller than the hard scale, since the effective scale entering the initial state collinear logarithms is damped by a kinematic factor which depends on the final state phase space. For charged Higgs boson production, the scale associated to the gluon splitting into bottom quarks is

$$\mathcal{Q}^2_{tHb} = M^2\frac{(1-z)^2}{z} \qquad \text{with} \qquad z = \frac{M^2}{\hat{s}}, \tag{5}$$

where $M^2 = (m_{H^\pm} + m_t)^2$ and $\hat{s}$ is the partonic centre-of-mass energy. By weighting this event-by-event logarithmic factor with the hard matrix element and the luminosity, a constant scale $\tilde{\mu}_f$ can be estimated which only depends on $m_{H^\pm}$, m_t and on the collider centre-of-mass energy $\sqrt{s}$. At this scale, the 5F scheme prediction can be meaningfully compared to the one in the 4F scheme [17]. The factorisation scale $\tilde{\mu}_f$ is presented in Table 1 for the full range of Higgs boson masses considered, for centre-of-mass energies of $\sqrt{s} = 8$ and 14 TeV.

	8 TeV		14 TeV	
$m_{H^\pm}$ (GeV)	$\tilde{\mu}_f$ (GeV)	$(m_{H^\pm}+m_t)/\tilde{\mu}_f$	$\tilde{\mu}_f$ (GeV)	$(m_{H^\pm}+m_t)/\tilde{\mu}_f$
200	68.9	5.5	76.3	4.9
220	70.7	5.6	79.6	4.9
240	73.4	5.6	82.7	5.0
260	75.9	5.7	85.9	5.0
280	78.5	5.8	89.0	5.1
300	81.0	5.8	92.0	5.1
320	83.5	5.9	95.0	5.2
340	85.9	6.0	97.9	5.2
360	88.3	6.0	100.9	5.3
380	90.7	6.1	103.8	5.3
400	93.0	6.2	106.6	5.4
420	95.3	6.2	109.4	5.4
440	97.5	6.3	112.2	5.5
460	99.7	6.3	115.0	5.5
480	101.9	6.4	117.7	5.5
500	104.0	6.5	120.4	5.6
520	106.2	6.5	123.1	5.6
540	108.2	6.6	125.7	5.7
560	110.3	6.6	128.3	5.7
580	112.3	6.7	130.9	5.7
600	114.3	6.7	133.4	5.8

Table 1: Dynamical factorisation scale $\tilde{\mu}_f$ for $pp \to tH^\pm + X$ for the LHC at $\sqrt{s} = 8$ and 14 TeV. The 4-flavour `CT10nlo_4f` PDF set has been used as input to evaluate $\tilde{\mu}_f$ according to Equation (5.13) of Reference [17].

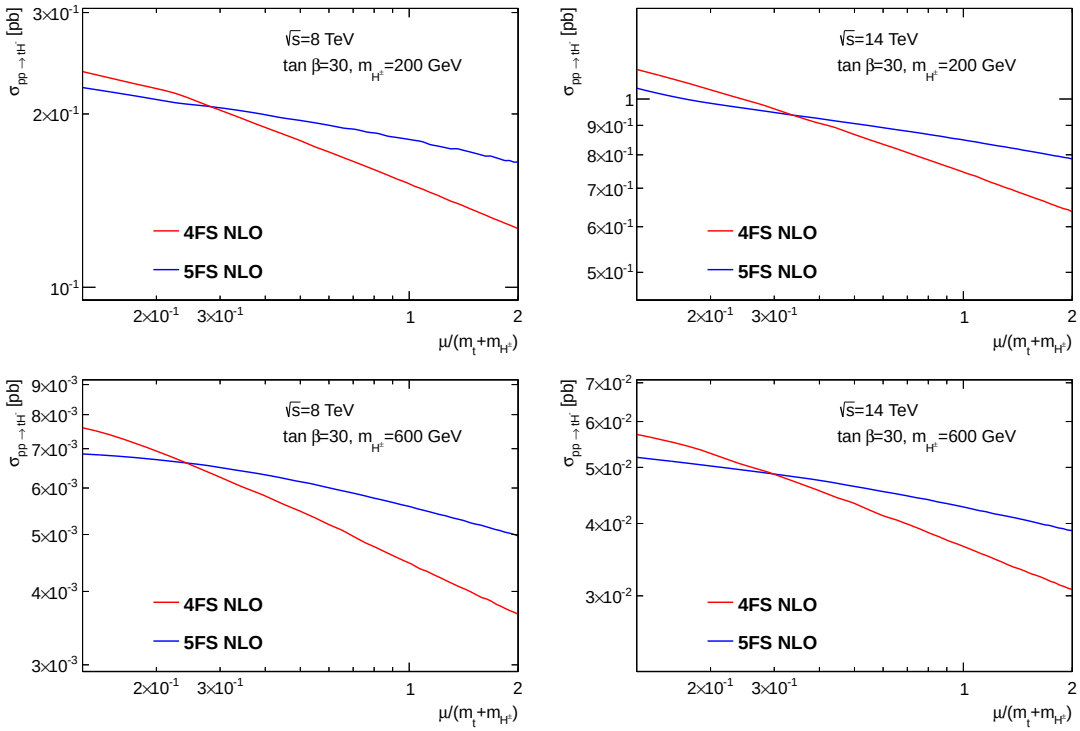

Figure 1: The dependence of the 4F and 5F scheme $pp \to tH^- + X$ total cross sections on the factorisation and renormalisation scales, for $m_H^\pm = 200$ (top) and 600 GeV (bottom) and $\sqrt{s} = 8$ TeV (left) and 14 TeV (right). Both scales are varied simultaneously between $\mu/10$ and 2μ about $(m_{H^\pm} + m_t)$.

The dependence of the total cross section on the renormalisation and factorisation scales is illustrated in Figure 1, for the largest and smallest $m_{H^\pm}$ values considered in this analysis. For the sake of illustration, the same value is used for both scales. This comparison, analogously to the one shown in References [17,60], is meant to illustrate the overall dependence of the total cross section on the scales that enter the computation. It is not meant to provide an exact estimate of the scale uncertainty. Both renormalisation and factorisation scales are varied between $\mu/10$ and 2μ around $(m_{H^\pm} + m_t)$, which is the natural hard scale of the process. For comparison, in Figure 1 the NLO scale dependence of the 4F calculation described in Section 4 is shown. The scale dependence of the 5F scheme calculation is milder than that of the 4F scheme calculation. The two calculations approach each other for scales smaller than $(m_{H^\pm} + m_t)$. Note that the choice of scale $\tilde{\mu}_f$ is not motivated by the argument illustrated in Figure 1, but the latter rather confirms the findings of the kinematical study that led to identify μ_f with $\tilde{\mu}_f$.

In the 5F scheme computation the three GM-VFNS PDF sets mentioned in Section 2 are used: the `CT10nlo` set [42] and the corresponding set with α_s variation, the `MSTW2008nlo68cl` set [43] and the corresponding sets with α_s and m_b variations, the `NNPDF23_nlo_as_0118` set [44] and the corresponding sets needed to compute the α_s and m_b variations. To illustrate the PDF uncertainty expected in the 5F scheme, the bottom-

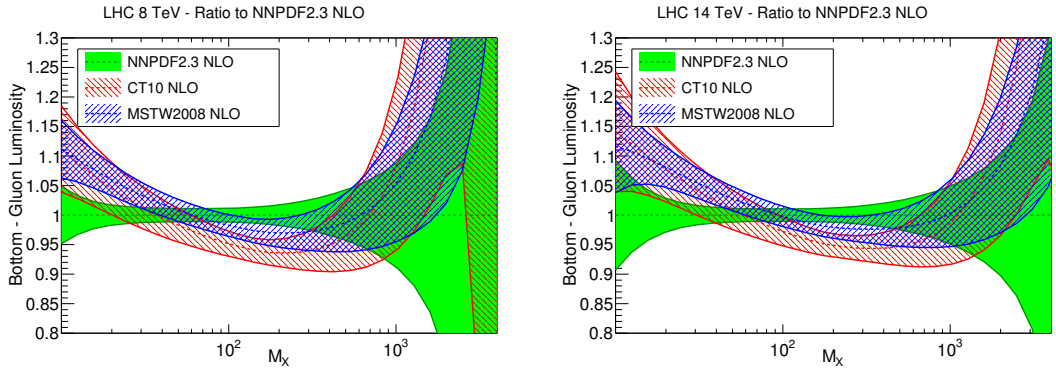

Figure 2: Gluon-bottom parton luminosities at the LHC for $\sqrt{s} = 8\,\text{TeV}$ (left) and $14\,\text{TeV}$ (right) for the default GM-VFN scheme NLO PDF sets CT10, MSTW2008 and NNPDF23, with $\alpha_s(M_Z) = 0.118$ and $m_b = 4.75\,\text{GeV}$. Uncertainties correspond to 68% C.L.

gluon luminosities for the three PDF sets, computed with $\alpha_s(M_Z) = 0.118$ and the default bottom quark mass $m_b = 4.75\,\text{GeV}$, are compared in Figure 2 for the LHC at $\sqrt{s} = 8\,\text{TeV}$ and $14\,\text{TeV}$. At a scale $M_X = m_{H^\pm} = 200\,\text{GeV}$ the 1σ error bands of the `NNPDF2.3` and `CT10` luminosities do not overlap, due to the harder gluon fitted by the NNPDF collaboration in the medium-to-large x region. At larger values of $m_{H^\pm}$ they tend to overlap, while at the same time the uncertainties become larger, driven by a larger gluon uncertainty at large values of x.

For each PDF set $\alpha_s(M_Z)$ is varied by 0.0012 around its central value [6]. The uncertainty due to the variation of $\alpha_s(M_Z)$ turns out to be negligible, its size being about a order of magnitude smaller than the PDF uncertainty. This is expected since the gluon and the bottom quark have opposite-sign correlation with the value of α_s in the region of x which is relevant for this process. Therefore a partial cancellation of the α_s dependence is expected.

The uncertainty associated to the value of the bottom quark pole mass used in the PDF fits is estimated by varying m_b in the range $m_b = 4.75 \pm 0.06\,\text{GeV}$.[4] In contrast to the α_s uncertainty, the m_b uncertainty induced by the PDFs is quite significant, corresponding to about 30-50% of the PDF uncertainty at fixed m_b. A significant dependence of the predicted cross section on the bottom quark mass has already been observed in several studies of processes initiated by bottom quarks [50,55,61] and has to be taken into account for a realistic estimate of the theoretical uncertainty.

Results are summarized in Table 2. The predictions obtained with `CT10` have the largest associated PDF uncertainty, as can be inferred from the luminosity plots in Figure 2. Furthermore, the size of the PDF uncertainty increases with the mass of the produced particles, the large-x region being the one in which the gluon and the bottom quark PDFs are least constrained by data. Compared to the PDF uncertainty, the relative m_b uncertainty is more significant for light charged Higgs boson masses ($m_{H^\pm} = 200\,\text{GeV}$),

[4] Note that CT10 provides sets to compute the PDF+α_s uncertainty, but does not provide sets associated to the m_b variation. Therefore, in contrast to MSTW2008 and NNPDF23, the CT10 uncertainty is underestimated.

$\sqrt{s}$ [TeV], PDF set	$m_{H^\pm}$ [GeV]	$\sigma_{\rm NLO}$ [pb]	$\delta_{\rm PDF}$ [%]	$\delta\alpha_s$ [%]	δm_b [%]
8	200	0.189	$^{+6.7}_{-6.0}$	$^{+0.6}_{-0.6}$	n.a.
CT10	400	0.0289	$^{+10.3}_{-\ 8.9}$	$^{+1.2}_{-1.2}$	n.a.
	600	0.00618	$^{+14.7}_{-11.7}$	$^{+1.9}_{-1.6}$	n.a.
8	200	0.195	$^{+4.7}_{-5.0}$	$^{+0.5}_{-0.4}$	$^{+2.8}_{-2.6}$
MSTW2008	400	0.0292	$^{+5.8}_{-7.9}$	$^{+0.7}_{-0.8}$	$^{+2.8}_{-2.7}$
	600	0.00609	$^{+8.3}_{-9.4}$	$^{+1.3}_{-1.2}$	$^{+2.9}_{-2.7}$
8	200	0.195	±4.4	±0.7	±1.2
NNPDF2.3	400	0.0288	±6.6	±0.6	±2.8
	600	0.00586	±8.9	±0.7	±1.5
14	200	0.870	$^{+3.9}_{-3.5}$	$^{+0.0}_{-0.0}$	n.a.
CT10	400	0.171	$^{+5.7}_{-5.2}$	$^{+0.0}_{-0.0}$	n.a.
	600	0.0458	$^{+7.6}_{-6.9}$	$^{+0.5}_{-0.5}$	n.a.
14	200	0.902	$^{+2.7}_{-3.6}$	$^{+0.1}_{-0.0}$	$^{+2.9}_{-2.7}$
MSTW2008	400	0.176	$^{+4.0}_{-3.9}$	$^{+0.0}_{-0.0}$	$^{+2.9}_{-2.6}$
	600	0.0468	$^{+4.7}_{-6.1}$	$^{+0.0}_{-0.2}$	$^{+2.9}_{-2.7}$
14	200	0.913	±2.7	±0.8	±1.5
NNPDF2.3	400	0.179	±3.9	±0.6	±1.2
	600	0.0471	±5.1	±0.5	±1.2

Table 2: Central value and PDF, α_s, m_b uncertainty for the next-to-leading order total $\bar{t}H^-$ production cross section in the 5F scheme, computed with different input PDF sets. Central values are computed with $\alpha_s(M_Z) = 0.118$, α_s variation by varying $\alpha_s(M_Z)$ by ±0.0012 about its central value, m_b variation by varying the m_b pole mass in the input PDFs by ±60 MeV. The n.a. in the boxes means that there is no available PDF set to compute the corresponding variation.

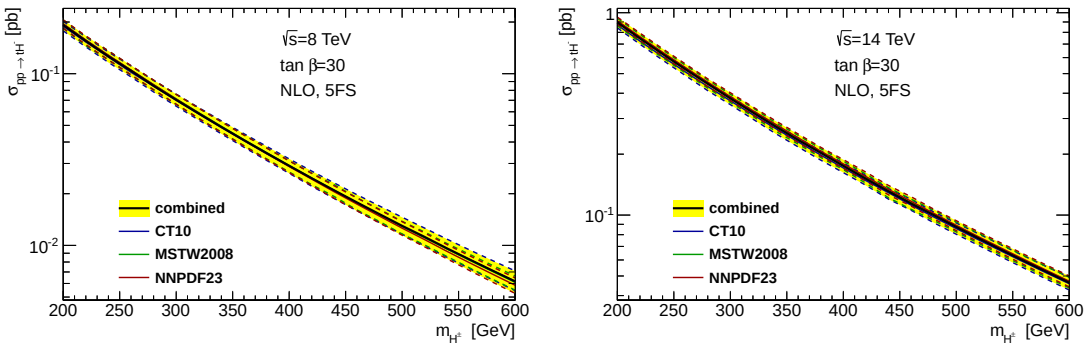

Figure 3: 5F scheme cross section and PDF+α_s+m_b uncertainty for $pp \to tH^\pm + X$ at the LHC with $\sqrt{s} = 8$ TeV (left) and 14 TeV (right), calculated with `CT10` (blue), `MSTW2008` (green) and `NNPDF23` (red) at NLO in a type-II 2HDM. The yellow band corresponds to the envelope of the three predictions.

with larger values of m_b corresponding to smaller cross sections. Note that there is a partial cancellation between the bottom quark mass dependence of the PDF and the Yukawa coupling which can be understood as follows: increasing the bottom quark mass in PDF fits reduces the phase space available for the splitting of gluons into bottom quarks and thus reduces the bottom PDF (a similar suppression is induced by the explicit logarithms of the bottom quark mass which appear in the 4F scheme calculation). Increasing the bottom quark mass in the Yukawa coupling, on the other hand, increases the Yukawa coupling and thus the cross-section normalization. For the overall bottom quark mass uncertainty, δm_b, reported in Table 2, the m_b dependence due to the PDF and due to the Yukawa coupling therefore partially cancel.

In Figure 3, the predictions for the total cross section are presented for each of the three PDF sets. The error band corresponds to the total PDF+α_s+m_b uncertainty, computed from the uncertainties shown in Table 2 according to Equation (3). Moreover the combined prediction is presented, i.e. the envelope of the total PDF+α_s+m_b uncertainty of each prediction, according to the PDF4LHC recommendation [62], and as described in Section 2. Taking the envelope significantly increases the size of the PDF uncertainty as obtained with each of the PDF sets individually, as it can also be inferred from Figure 2.

Finally the scale uncertainty due to missing higher orders, $\Delta^{\pm}_{\mu}$, obtained according to the prescription described in Section 2, is linearly added to upper and lower bounds of the envelope, according to Equation (4). The variation of the renormalisation scale and the scale in the Yukawa coupling contribute approximately equally to $\Delta^{\pm}_{\mu}$, while the impact of the factorisation scale dependence is smaller by about a factor of two. All individual sources of uncertainty, scale variation and total PDF uncertainty (including α_s and m_b variation) are listed in Table 3.

Figure 4 displays the combined cross section, with its total theoretical uncertainty split up into PDF+α_s+m_b uncertainty and scale variation. For the charged Higgs boson mass range considered, the size of the two uncertainties is comparable, with the total PDF uncertainty being larger for higher $m_{H^\pm}$ masses.

$\sqrt{s}$ [TeV]	$m_{H^\pm}$ [GeV]	σ_{NLO} [pb]	$\Delta^\pm_\mu$ [%]	$\delta^\pm_{\text{PDF}+\alpha_s+m_b}$ [%]	$\Delta^\pm_{\text{tot}}$ [%]
8	200	0.192	$^{+9.4}_{-9.4}$	± 7.3	$^{+16.7}_{-16.7}$
	400	0.0291	$^{+9.3}_{-8.6}$	± 9.6	$^{+18.9}_{-18.2}$
	600	0.00617	$^{+9.4}_{-8.9}$	± 14.9	$^{+24.3}_{-23.8}$
14	200	0.895	$^{+9.8}_{-9.7}$	± 6.3	$^{+16.1}_{-16.0}$
	400	0.175	$^{+8.6}_{-8.6}$	± 7.3	$^{+15.9}_{-15.9}$
	600	0.0463	$^{+8.4}_{-8.4}$	± 8.0	$^{+16.4}_{-16.4}$

Table 3: Central prediction, scale uncertainty, PDF+α_s+m_b uncertainty, and total theoretical uncertainty for the next-to-leading order tH^- production cross section in the 5F scheme.

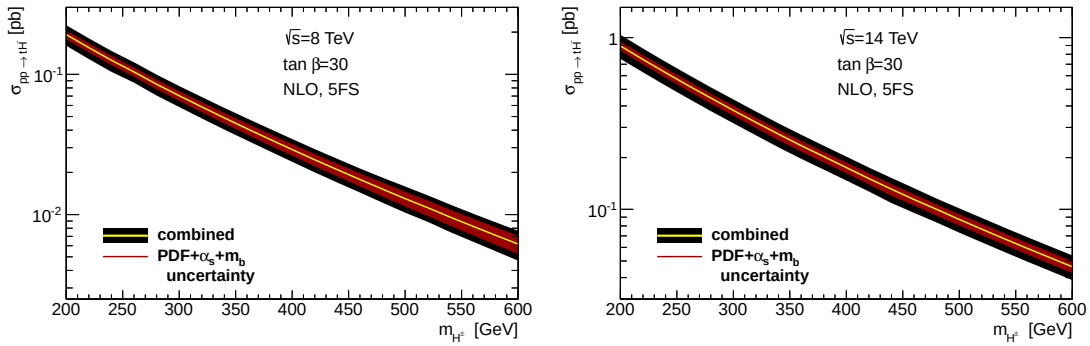

Figure 4: 5F cross section and uncertainties for $pp \to tH^\pm + X$ for the LHC at $\sqrt{s} = 8\,\text{TeV}$ (left) and 14 TeV (right). Shown is the combined central value and the total uncertainty, split up into PDF+α_s+m_b and scale uncertainties.

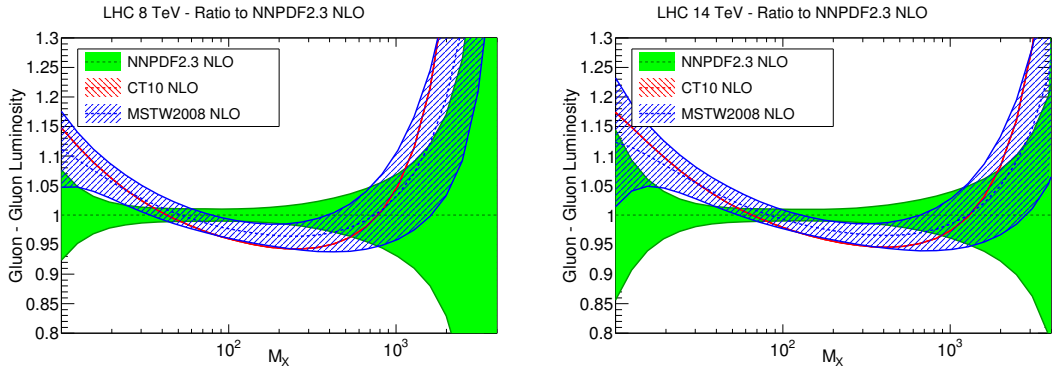

Figure 5: Gluon-gluon parton luminosities at the LHC at $\sqrt{s} = 8\,\text{TeV}$ (left) and $14\,\text{TeV}$ (right) for the 4F Fixed-Flavour-Number NLO PDF sets provided by CT10, MSTW2008 and NNPDF23, with the default α_s^{4F} and m_b values provided by each collaboration. Uncertainties are at 68% C.L.

4 Four-flavour scheme results

In the 4F scheme, bottom quarks are created perturbatively in the hard part of the process, and the bottom quark mass is included exactly at all orders. At leading order the partonic processes are given by

$$q\bar{q}, gg \quad \longrightarrow \quad tH^-\bar{b},$$

while next-to-leading order QCD corrections consists of virtual one-loop diagrams, gluon radiation and gluon (anti-)quark scattering [12]. The total theoretical uncertainty of the 4F prediction is estimated according to Equation (4). The dependence of the NLO cross section on the factorisation and renormalisation scales is illustrated in Figure 1. The scale uncertainty estimate is obtained by varying μ_r, μ_f and μ_b by a factor two about their central values $\mu = (m_{H^\pm} + m_t + m_b)/3$, as described in Section 2.

In the 4F scheme cross-section calculation the fixed-flavour-number PDF sets with $n_f = 4$ provided by the global PDF fitting collaborations are used. The corresponding gluon-gluon luminosities are shown in Figure 5. Here, it is not possible to evaluate the PDFs at a common value of α_s since only the NNPDF collaboration provides FFN sets computed at various values of $\alpha_s^{4F}(M_z)$, while the MSTW and the CT collaborations only provide 4F PDF sets at their default α_s values, $\alpha_s^{4F}(M_z) = 0.1149$ for `MSTW2008nlo68cl_nf4` and $\alpha_s^{4F}(M_z) = 0.1127$ for `CT10nlo_nf4`. Moreover CT10 do not provide an estimate of the PDF uncertainty for their $n_f = 4$ set. This leads to a slight underestimate in the total PDF uncertainty based on the envelope of the three predictions. In the charged Higgs boson mass range considered in this analysis the NNPDF2.3 and the MSTW2008 gluon-gluon luminosities barely overlap within their 1σ error bar and the CT10 central curve lies at the bottom of the MSTW curve. This behaviour reflects the features observed in Figure 2, as a consequence of the correlation between the bottom and the gluon PDFs.

Since the `MSTW200868cl_nf4` sets are provided at several values of m_b it is possible to estimate the PDF+m_b uncertainty for the 4F predictions by varying m_b in the input PDF sets and in the hard matrix element. The variation of the pole m_b mass in a 4F

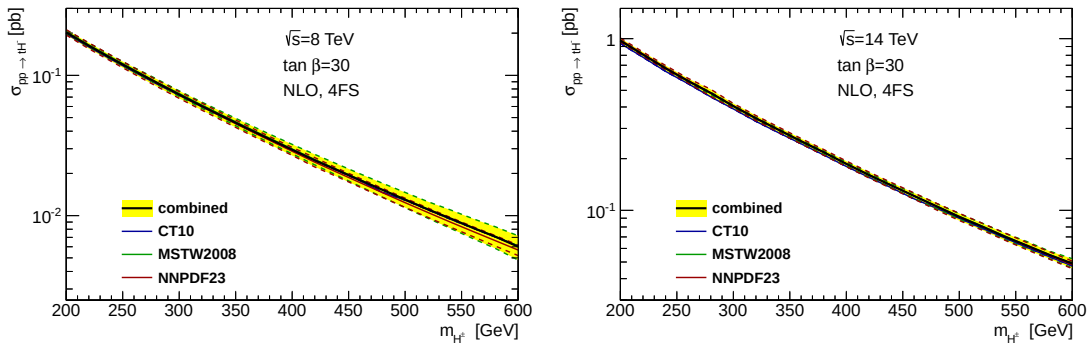

Figure 6: 4F scheme cross section and PDF+α_s+m_b uncertainty for $pp \to tH^{\pm} + X$ at the LHC with $\sqrt{s} = 8$ and 14 TeV , calculated with `CT10` (blue), `MSTW2008` (green) and `NNPDF23` (red) at NLO in a type-II 2HDM. The yellow band corresponds to the envelope of the three predictions.

scheme PDF set is expected to have little influence, as m_b only enters the partonic DIS cross section fitted in the global fit of PDFs. The major dependence on m_b comes from the variation of m_b in the hard matrix element through the collinear logarithm.

On the other hand, the `NNPDF2.3` FFN sets are given at several values of α_s and this allows to estimate the PDF+α_s uncertainty of the 4F prediction. It turns out that the α_s uncertainty contributes very little to the total uncertainty while the m_b variation induces an additional uncertainty in the theoretical predictions which is small but not negligible compared to the PDF error band.

Results are collected in Table 4, in which the relative uncertainty for each contribution is reported. The central value for the next-to-leading order cross section computed in the 4F scheme predicted by using the CT10 set is always smaller with respect to the predictions obtained with MSTW or NNPDF2.3, partially because the α_s^{4F} of the CT10 fit is smaller than that of the other PDFs. Furthermore, the PDF uncertainty increases as the mass of the produced Higgs boson increases, a consequence of the rise in the gluon uncertainty at large x. A comparison of the predicted cross section for the full range of charged Higgs boson masses considered is shown in Figure 6. The large uncertainty of the MSTW2008 gluon at large x is at the origin of the large PDF uncertainty at large $m_{H^{\pm}}$ masses at $\sqrt{s} = 8$ TeV. At larger hadronic centre-of-mass energies, the gluon distributions peak at a smaller value of x where the PDF uncertainty is less pronounced. Note that for large Higgs boson masses the average parton momentum fraction x, and thus the PDF uncertainty, is larger in the 4FS than in the 5FS.

Finally the uncertainty due to missing higher order contributions is linearly added to upper and lower bounds of the envelope, according to Equation (4). Note that the scale in the running m_b mass in the Yukawa coupling contributes significantly to the scale variation, and contributes about 5 percentage points to the total scale uncertainty of 15% to 20% in the range of Higgs boson masses considered. Neglecting the μ_b variation would therefore lead to an underestimate of the scale uncertainty. All individual sources of uncertainty - scale variation, total PDF uncertainty (including α_s and m_b variation) and

$\sqrt{s}$[TeV], PDF set	$m_{H^\pm}$[GeV]	$\sigma_{\rm NLO}$ [pb]	$\delta_{\rm PDF}$ [%]	$\delta\alpha_s$ [%]	δm_b [%]
8	200	0.198	n.a	n.a.	n.a.
CT10	400	0.0293	n.a	n.a.	n.a.
	600	0.00608	n.a	n.a.	n.a.
8	200	0.205	$^{+2.3}_{-2.7}$	n.a.	$^{+0.5}_{-0.5}$
MSTW2008	400	0.0299	$^{+7.9}_{-7.6}$	n.a.	$^{+0.5}_{-0.5}$
	600	0.00610	$^{+17.8}_{-20.8}$	n.a.	$^{+0.5}_{-0.5}$
8	200	0.203	± 4.3	$^{+1.1}_{-0.8}$	n.a.
NNPDF2.3	400	0.0288	± 6.4	$^{+0.8}_{-1.2}$	n.a.
	600	0.00569	± 8.4	$^{+0.8}_{-2.2}$	n.a.
14	200	0.938	n.a	n.a.	n.a.
CT10	400	0.180	n.a.	n.a.	n.a.
	600	0.0475	n.a.	n.a.	n.a.
14	200	0.972	$^{+1.1}_{-0.8}$	n.a.	$^{+0.5}_{-0.4}$
MSTW2008	400	0.186	$^{+2.2}_{-2.7}$	n.a.	$^{+0.4}_{-0.4}$
	600	0.0489	$^{+6.9}_{-5.5}$	n.a.	$^{+0.3}_{-0.6}$
14	200	0.983	± 2.6	$^{+0.1}_{-0.0}$	n.a.
NNPDF2.3	400	0.187	± 3.8	$^{+0.4}_{-0.5}$	n.a.
	600	0.0481	± 5.0	$^{+0.6}_{-0.9}$	n.a.

Table 4: Central value and PDF, α_s, m_b uncertainties for the next-to-leading order total tH^- production cross section in the 4F scheme, computed with different input PDF sets. Central values are computed with the default value of $\alpha_s(M_Z)$ provided by each PDF set, α_s variation by varying $\alpha_s(M_Z)$ by ± 0.0012 about its central value, m_b variation by varying the m_b pole mass in the input PDFs and in the hard matrix element by ± 60 MeV. The n.a. in the boxes means that there is no available PDF set to compute the corresponding variation.

$\sqrt{s}$[TeV]	$m_{H^\pm}$[GeV]	σ_{NLO} [pb]	$\Delta^\pm_\mu$ [%]	$\delta^\pm_{\text{PDF}+\alpha_s+m_b}$ [%]	$\Delta^\pm_{\text{tot}}$ [%]
8	200	0.202	$^{+18.2}_{-20.1}$	± 4.4	$^{+22.6}_{-24.5}$
	400	0.0295	$^{+20.6}_{-21.3}$	± 9.2	$^{+29.8}_{-30.4}$
	600	0.00601	$^{+23.7}_{-22.0}$	± 19.6	$^{+43.4}_{-41.6}$
14	200	0.973	$^{+16.8}_{-17.5}$	± 3.6	$^{+20.4}_{-21.1}$
	400	0.187	$^{+17.7}_{-18.4}$	± 3.8	$^{+21.5}_{-22.2}$
	600	0.0491	$^{+19.4}_{-18.7}$	± 6.6	$^{+25.9}_{-25.3}$

Table 5: Central prediction, scale uncertainty, PDF+α_s+m_b uncertainty, and total theoretical uncertainty for the next-to-leading order tH^- production cross section in the 4F scheme.

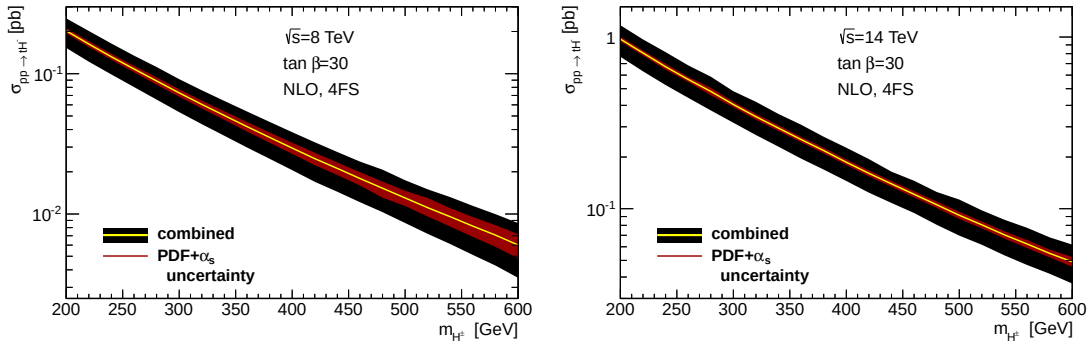

Figure 7: 4F cross section and uncertainties for $pp \to tH^\pm + X$ for the LHC at $\sqrt{s} = 8\,\text{TeV}$ (left) and 14 TeV (right). Shown is the combined central value and the total uncertainty, split up into PDF+α_s+m_b and scale uncertainties.

total uncertainty - are listed in Table 5. The results in the table show that overall the scale uncertainty is the dominating source of theoretical uncertainty for lower $m_{H^\pm}$ masses. The same can be observed in Figure 7 in which the central prediction for the 4F scheme cross section is presented, with its uncertainty split up into scale and PDF+α_s+m_b uncertainties. At large $m_{H^\pm}$ masses, especially at 8 TeV, the large x gluon uncertainty drives the total theoretical uncertainty above 40%. The release of PDF sets that include the constraints from the precise LHC jet and top data will help in reducing the uncertainty of the gluons at large x and consequently decrease the uncertainty of the theoretical predictions.

5 Comparison and matching

The 4F and 5F schemes only yield identical results for the $pp \to tH^\pm + X$ cross sections in an all-order calculation, as was shown for instance in Reference [45]. At finite order, the schemes include different contributions, since the perturbative expansion is ordered

differently. Thus, the predictions within the two schemes can be used to cross-check results, and to estimate the impact of neglected contributions at higher order.

To obtain a unique theoretical prediction which can be confronted with experimental data, the 4F and 5F schemes can be combined using a prescription called Santander-matching [28]. In the asymptotic limits $m_{H^\pm}/m_b \to 1$ and $m_{H^\pm}/m_b \to \infty$, the 4F and 5F schemes, respectively, provide the unique description of the cross section. For realistic Higgs boson masses in the range from 200 GeV to 600 GeV considered here, both schemes contribute with a given finite weight which depends on the charged Higgs boson mass [28]. The difference between the two approaches is formally logarithmic, and thus the dependence of their relative importance on the Higgs boson is determined by a logarithmic term, i.e.

$$\sigma_{\text{matched}} = \frac{\sigma_{\text{4F}} + w\sigma_{\text{5F}}}{1+w}\,, \tag{6}$$

with the weight w defined as

$$w = \log\frac{m_{H^\pm}}{m_b} - 2\,. \tag{7}$$

This yields a weight of 100% for the 5F-scheme cross section σ_{5F} in the limit of $m_{H^\pm}/m_b \to \infty$ as desired. A weight of 50% is given to both cross sections for $m_{H^\pm}$ around 100 GeV, to reflect the observation that predictions for both schemes agree well in this region. The theoretical uncertainties are combined as

$$\Delta\sigma^{\pm}_{\text{tot,matched}} = \frac{\Delta\sigma^{\pm}_{\text{tot,4F}} + w\Delta\sigma^{\pm}_{\text{tot,5F}}}{1+w}\,. \tag{8}$$

The Santander-matching scheme is a pragmatic and simple approach to derive a unique prediction from the 4F and 5F scheme results, and not based on a thorough field-theoretic analysis. However, the Santander-matched results encompass the essential features of the the two schemes. The corresponding matched predictions and uncertainty estimates are expected to be close to the true cross section, in particular as the 4F and 5F scheme calculations for heavy charged Higgs boson production with the improved scale setting prescription are in good mutual agreement.

The cross section and uncertainty for the results of the 4F and 5F scheme calculations and their combination for $\sqrt{s} = 8$ and 14 TeV are presented in Figure 8. The predictions from both schemes agree well within their uncertainties, with differences of at most 10%. The prediction [17] that the impact of the resummation of the collinear logarithms decreases for higher masses of the produced heavy particle is confirmed. The overall theoretical uncertainty of the matched NLO prediction is about 20–30%, very close to the 5F uncertainty that, for the considered range of masses, has a larger weight.

A much better agreement than in earlier comparisons [12] is observed. There, the choice for the factorisation scale in the 5F-scheme was $\mu_f = (m_t + m_{H^\pm})/3$. The dynamical choice for μ_f used here significantly improves the agreement between the predictions in the two schemes. In addition the improved treatment of threshold effects in the modern PDF sets employed here has lead to a decrease of the bottom PDFs compared to previous analyses, and has thus moved the 5F scheme calculation closer to the 4F cross section prediction.

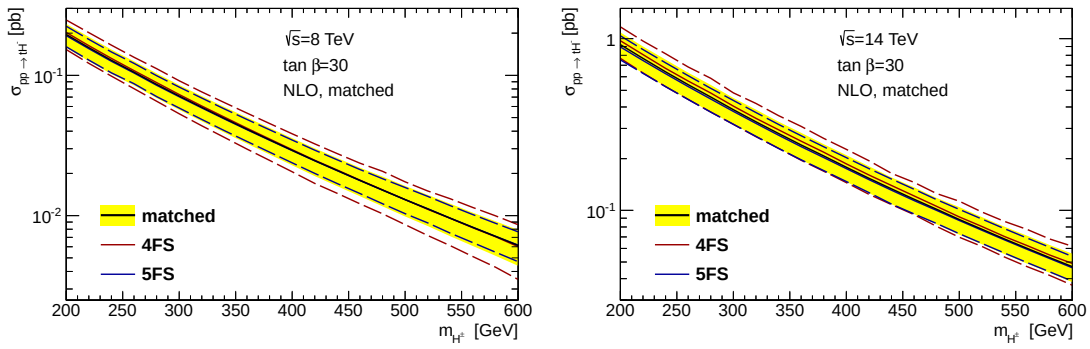

Figure 8: Santander-matched cross section and uncertainties for $pp \to tH^{\pm} + X$ at the LHC for 8 and 14 TeV. The 4F and 5F scheme results as well as the combined values are shown, together with their total uncertainties.

6 Varying the parameter $\tan\beta$

The cross section for charged Higgs boson production in association with a top quark and a bottom quark depends on the ratio of the vacuum expectation values of the two Higgs doublets, $\tan\beta = v_2/v_1$, through the Yukawa coupling, see Equation (2). The Yukawa coupling consists of two pieces which scale as $\tan\beta$ and $\cot\beta$, respectively. Thus changing $\tan\beta$ induces a non-trivial change in the cross section, but also in the theoretical uncertainty. First, the scale dependence as a function of $\tan\beta$ is considered for two values of the charged Higgs boson mass and the centre-of-mass energies 8 and 14 TeV in Figure 9. A relatively uniform behavior is observed where the scale dependence decreases with decreasing $\tan\beta$ from about 20% to 15% and 10% to 5% for the 4F and 5F scheme calculations, respectively. This is caused by the decreasing relevance of the running bottom Yukawa coupling, which is proportional to $\tan\beta$ and which adds about 5 percentage points to the overall scale uncertainty for large $\tan\beta$.

The NLO cross sections in the 4F and 5F schemes and in the Santander-matched calculation are displayed in Figure 10 for the LHC at $\sqrt{s} = 14$ TeV. The total cross section is essentially proportional to the size of the $tbH^{\pm}$ coupling which has a minimum for $\tan\beta \approx 8$. Comparing the 4F and 5F scheme calculations, both agree over the whole range of $\tan\beta$ although the difference in the central values is slightly larger for small $\tan\beta$. In this region, the results become sensitive to the top-bottom-Yukawa interference term $\propto m_t\, m_b$, which is absent in the 5FS calculation.

In a type-I 2HDM all quarks couple to only one of the Higgs doublets. In such models, the Yukawa coupling of the charged Higgs boson H^- to a top quark and bottom antiquark is given by

$$g_{t\bar{b}H^-}|_{\text{type-I}} = \sqrt{2}\left(\frac{m_t}{v} P_R \cot\beta - \frac{m_b}{v} P_L \cot\beta\right). \tag{9}$$

In contrast to the type-II 2HDM, for type-I the bottom Yukawa coupling is not enhanced by $\tan\beta$, so that $g_{t\bar{b}H^-}|_{\text{type-I}} = \sqrt{2}\, m_t/v\, P_R \cot\beta + \mathcal{O}(m_b/m_t)$. Up to corrections suppressed by $\mathcal{O}(m_b/m_t)$, the cross section for heavy charged Higgs boson production in the type-I 2HDM, $\sigma|_{\text{type-I}} \propto g^2_{t\bar{b}H^-}|_{\text{type-I}} \propto 2(m_t/v)^2 \cot^2\beta + \mathcal{O}(m_b/m_t)$, can thus be obtained from

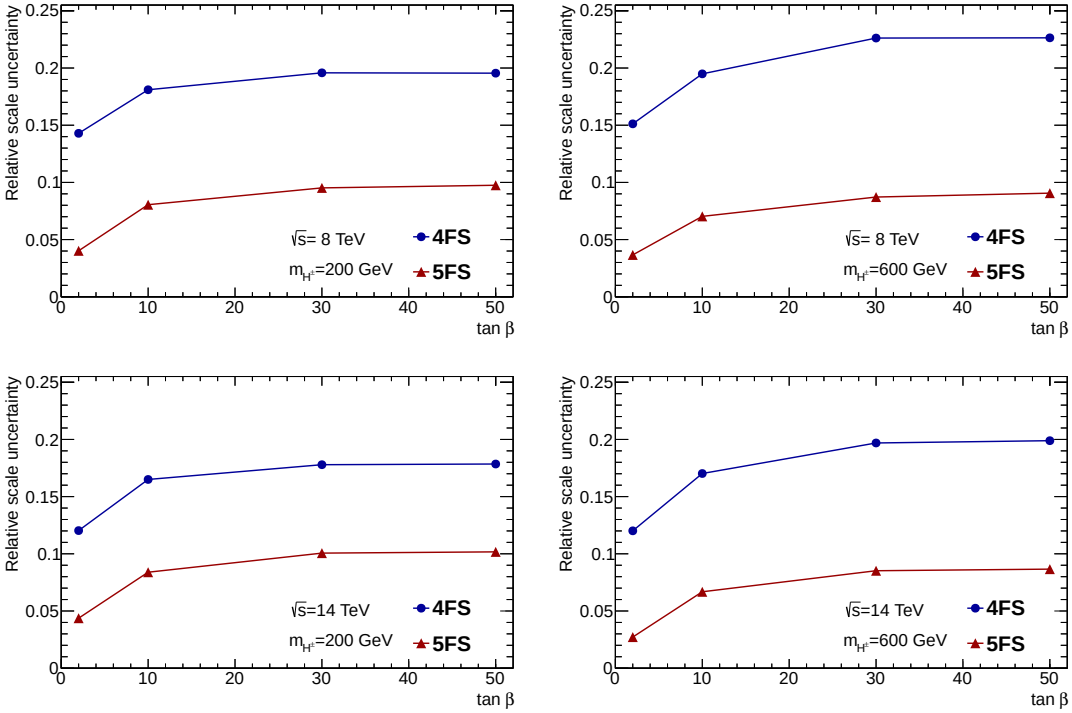

Figure 9: Scale dependence as a function of $\tan\beta$ for the 4F and 5F predictions for the LHC at $\sqrt{s} = 8\,\text{TeV}$ (top row) and $\sqrt{s} = 14\,\text{TeV}$ (bottom row) for two values of $m_{H^\pm}$ masses: 200 GeV (left) and 600 GeV (right).

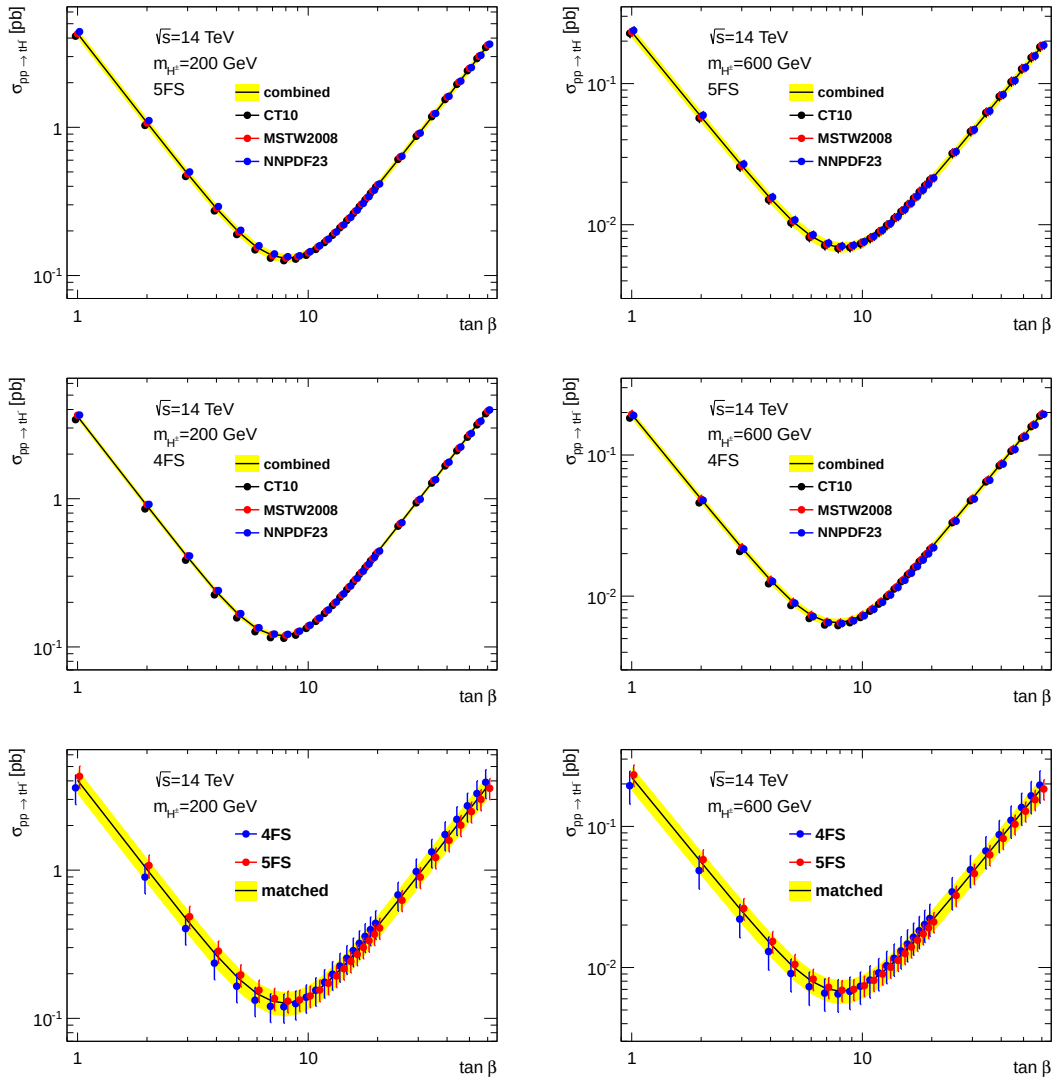

Figure 10: The $pp \to tH^- + X$ cross section as a function of $\tan\beta$. Shown are the 5F scheme calculation (top row), the 4F scheme calculation (middle row) and the matched calculation (bottom row) for the LHC at $\sqrt{s} = 14$ TeV for a charged Higgs boson mass of 200 GeV (left column) and 600 GeV (right column). The upper two rows show the PDF+α_s+m_b uncertainties while for the bottom row, the scale uncertainties are included as well.

the type-II cross section, $\sigma|_{\text{type-II},\tan\beta=1} \propto g^2_{t\bar{b}H^-}|_{\text{type-II},\tan\beta=1} \propto 2(m_t/v)^2 + \mathcal{O}(m_b/m_t)$, evaluated at $\tan\beta = 1$ and rescaled by $\cot^2\beta$. This relation is correct to all orders in QCD, but *not* to all orders in the electroweak corrections. Given the overall theoretical uncertainty of the cross-section prediction of $\mathcal{O}(30\%)$ it is, however, an excellent approximation and sufficient for all practical purposes. Note that the charged Higgs boson cross-section predictions for the type-I and type-II 2HDMs also hold for the so-called lepton-specific and flipped 2HDMs, respectively, see e.g. Reference [63].

7 Conclusions

An updated and improved NLO-QCD calculation of the associated production of a heavy charged Higgs boson at the LHC within a type-II two-Higgs-doublet model has been presented. The improvements with respect to previous NLO predictions include adopting a new scale setting procedure for the five-flavour scheme, a thorough treatment of the theoretical uncertainties based on state-of-the-art PDF sets, and a matched prediction for the four- and five-flavour scheme calculations.

The dynamical choice of the factorisation scale in the five-flavour scheme calculation significantly improves the agreement between the four- and five-flavour schemes. The overall uncertainty of the matched cross-section prediction is approximately 20–30%, and includes the dependence on the renormalisation scale, the factorisation scale, the scale of the running bottom quark mass in the Yukawa coupling, as well as the input parameter uncertainties in the parton distribution functions, in the QCD coupling α_s, and in the bottom quark mass. The scale dependence and the input parameter uncertainties contribute about equally to the overall uncertainty.

The NLO-QCD cross-section prediction is provided as a function of $m_{H^\pm}$ and $\tan\beta$, and a simple yet accurate prescription is presented to convert the result to the production of heavy charged Higgs bosons in type-I , and in so-called lepton-specific and flipped two-Higgs-doublet models. The numerical results are made available through the wiki page of the LHC Higgs Cross Section working group [64], and allow the interpretation of LHC searches for heavy charged Higgs bosons for a wide class of beyond-the-SM scenarios.

Acknowledgements

The authors would like to thank Stefan Dittmaier, Fabio Maltoni, Tilman Plehn and Giovanni Ridolfi for useful discussions and comments. MK is grateful to SLAC and Stanford University for their hospitality. The work of MK has been supported by the DFG SFB/TR9 "Computational Particle Physics" and by the U.S. Department of Energy under contract DE-AC02-76SF00515. The work of M.S. is supported in part by the European Commission through the HiggsTools Initial Training Network PITN-GA-2012-316704. The work of M.U. is supported by the UK Science and Technology Facilities Council.

References

[1] G. Abbiendi et al. Search for Charged Higgs bosons: Combined Results Using LEP Data. Eur.Phys.J., C73:2463, 2013.

[2] T. Aaltonen et al. Search for charged Higgs bosons in decays of top quarks in p-pbar collisions at $\sqrt{s} = 1.96$ TeV. Phys. Rev. Lett., 103:101803, 2009.

[3] V. M. Abazov et al. Search for charged Higgs bosons in top quark decays. Phys. Lett. B, 682:278, 2009.

[4] ATLAS Collaboration. Search for charged Higgs bosons in the τ+jets final state with pp collision data recorded at $\sqrt{s} = 8$ TeV with the ATLAS experiment. ATLAS-CONF-2013-090, 2013.

[5] CMS Collaboration. Search for a light charged Higgs boson in top quark decays in pp collisions at $\sqrt{s} = 7$ TeV. JHEP, 1207:143, 2012.

[6] J. Behringer et al. (Particle Data Group). 2012 Review of Particle Physics. Phys.Rev., D86, 2012.

[7] R. M. Barnett, H. E. Haber, and D. E. Soper. Ultraheavy Particle Production from Heavy Partons at Hadron Colliders. Nucl. Phys., B306:697, 1988.

[8] D. A. Dicus and S. Willenbrock. Higgs Boson Production from Heavy Quark Fusion. Phys. Rev., D39:751, 1989.

[9] W. Tung, S. Kretzer, and C. Schmidt. Open heavy flavor production in QCD: Conceptual framework and implementation issues. J.Phys., G28:983–996, 2002.

[10] J. M. Campbell, S. Dawson, S. Dittmaier, C. Jackson, M. Kramer, et al. Higgs boson production in association with bottom quarks. arXiv:hep-ph/0405302, 2004.

[11] D. L. Rainwater, M. Spira, and D. Zeppenfeld. Higgs boson production at hadron colliders: Signal and background processes. arXiv:hep-ph/0203187, 2002.

[12] S. Dittmaier, M. Kramer, M. Spira, and M. Walser. Charged-Higgs-boson production at the LHC: NLO supersymmetric QCD corrections. Phys.Rev., D83:055005, 2011.

[13] E. Boos and T. Plehn. Higgs-boson production induced by bottom quarks. Phys. Rev., D69:094005, 2004.

[14] F. Maltoni, Z. Sullivan, and S. Willenbrock. Higgs-boson production via bottom-quark fusion. Phys. Rev., D67:093005, 2003.

[15] M. Kramer. Charged Higgs boson production at the LHC. PoS, CHARGED2010:025, 2010.

[16] S. Dittmaier, M. Kramer, M. Spira, and M. Walser. Associated charged higgs production with heavy quarks: SUSY QCD corrections. PoS, RADCOR2009:046, 2010.

[17] F. Maltoni, G. Ridolfi, and M. Ubiali. b-initiated processes at the LHC: a reappraisal. JHEP, 1207:022, 2012.

[18] T. Plehn. Charged Higgs boson production in bottom gluon fusion. Phys.Rev., D67:014018, 2003.

[19] S. Dawson, A. Ismail, and I. Low. A Redux on "When is the Top Quark a Parton?". arXiv:1405.6211, 2014.

[20] S. Zhu. Complete next-to-leading order QCD corrections to charged Higgs boson associated production with top quark at the CERN large hadron collider. Phys.Rev., D67:075006, 2003.

[21] G. Gao, G. Lu, Z. Xiong, and J. Yang. Loop effects and nondecoupling property of SUSY QCD in $gb \to tH$. Phys.Rev., D66:015007, 2002.

[22] E. L. Berger, T. Han, J. Jiang, and T. Plehn. Associated production of a top quark and a charged Higgs boson. Phys.Rev., D71:115012, 2005.

[23] N. Kidonakis. Charged Higgs production: Higher-order corrections. PoS, HEP2005:336, 2006.

[24] C. Weydert, S. Frixione, M. Herquet, M. Klasen, E. Laenen, et al. Charged Higgs boson production in association with a top quark in MC@NLO. Eur.Phys.J., C67:617–636, 2010.

[25] W. Peng, M. Wen-Gan, Z. Ren-You, J. Yi, H. Liang, et al. NLO supersymmetric QCD corrections to the $t\bar{b}H^-$ associated production at hadron colliders. Phys.Rev., D73:015012, 2006.

[26] M. Beccaria, G. Macorini, L. Panizzi, F.M. Renard, and C. Verzegnassi. Associated production of charged Higgs and top at LHC: The Role of the complete electroweak supersymmetric contribution. Phys.Rev., D80:053011, 2009.

[27] Dao Thi Nhung, Wolfgang Hollik, and Le Duc Ninh. Electroweak corrections to $gg \to H^- t\bar{b}$ at the LHC. Phys.Rev., D87(11):113006, 2013.

[28] R. Harlander, M. Kramer, and M. Schumacher. Bottom-quark associated Higgs-boson production: reconciling the four- and five-flavour scheme approach. CERN-PH-TH-2011-134, 2011.

[29] LHC Higgs cross section working group. `https://twiki.cern.ch/twiki/bin/view/LHCPhysics/LHCHXSWG`.

[30] LHC Higgs Cross Section Working Group, S. Heinemeyer, C. Mariotti, G. Passarino, and R. Tanaka (Eds.). Handbook of LHC Higgs Cross Sections: 3. Higgs Properties. CERN-2013-004, 2013.

[31] M. S. Carena, M. Olechowski, S. Pokorski, and C.E.M. Wagner. Radiative electroweak symmetry breaking and the infrared fixed point of the top quark mass. Nucl.Phys., B419:213–239, 1994.

[32] D. M. Pierce, J. A. Bagger, K. T. Matchev, and R. Zhang. Precision corrections in the minimal supersymmetric standard model. Nucl.Phys., B491:3–67, 1997.

[33] R. Hempfling. Yukawa coupling unification with supersymmetric threshold corrections. Phys.Rev., D49:6168–6172, 1994.

[34] L. J. Hall, R. Rattazzi, and U. Sarid. The Top quark mass in supersymmetric SO(10) unification. Phys.Rev., D50:7048–7065, 1994.

[35] J. Guasch, P. Hafliger, and M. Spira. MSSM Higgs decays to bottom quark pairs revisited. Phys.Rev., D68:115001, 2003.

[36] M. S. Carena, D. Garcia, U. Nierste, and C. E.M. Wagner. Effective Lagrangian for the $\bar{t}bH^+$ interaction in the MSSM and charged Higgs phenomenology. Nucl.Phys., B577:88–120, 2000.

[37] D. Noth and M. Spira. Supersymmetric Higgs Yukawa Couplings to Bottom Quarks at next-to-next-to-leading Order. JHEP, 1106:084, 2011.

[38] D. Noth and M. Spira. Higgs Boson Couplings to Bottom Quarks: Two-Loop Supersymmetry-QCD Corrections. Phys.Rev.Lett., 101:181801, 2008.

[39] L. Mihaila and C. Reisser. $O(\alpha_s^2)$ corrections to fermionic Higgs decays in the MSSM. JHEP, 1008:021, 2010.

[40] B.C. Allanach, M. Battaglia, G.A. Blair, Marcela S. Carena, A. De Roeck, et al. The Snowmass points and slopes: Benchmarks for SUSY searches. Eur.Phys.J., C25:113–123, 2002.

[41] M.R. Whalley, D. Bourilkov, and R.C. Group. The Les Houches accord PDFs (LHAPDF) and LHAGLUE. arXiv:hep-ph/0508110, 2005.

[42] H. Lai, M. Guzzi, J. Huston, Z. Li, P. M. Nadolsky, et al. New parton distributions for collider physics. Phys.Rev., D82:074024, 2010.

[43] A.D. Martin, W.J. Stirling, R.S. Thorne, and G. Watt. Parton distributions for the LHC. Eur.Phys.J., C63:189–285, 2009.

[44] R. D. Ball, V. Bertone, S. Carrazza, C. S. Deans, L. Del Debbio, et al. Parton distributions with LHC data. Nucl.Phys., B867:244–289, 2013.

[45] M.A.G. Aivazis, J.C. Collins, F.I. Olness, W.-K. Tung. Leptoproduction of heavy-quarks. 2. A Unified QCD formulation of charged and neutral current processes from fixed target collider energies. Phys.Rev., D50:3102–3118, 1994.

[46] R.S. Thorne, R.G. Roberts. An ordered analysis of heavy flavor production in deep inelastic scattering. Phys.Rev., D57:6871–6898, 1998.

[47] R.S. Thorne. A Variable-flavor number scheme for NNLO. Phys.Rev., D73:054019, 2006.

[48] M. Cacciari, M. Greco, P. Nason. The p(T) spectrum in heavy flavour hadroproduction. JHEP, 9805:007, 1998.

[49] S. Forte, E. Laenen, P. Nason, and J. Rojo. Heavy quarks in deep-inelastic scattering. Nucl.Phys., B834:116–162, 2010.

[50] A.D. Martin, W.J. Stirling, R.S. Thorne, and G. Watt. Heavy-quark mass dependence in global PDF analyses and 3- and 4-flavour parton distributions. Eur.Phys.J., C70:51–72, 2010.

[51] R. D. Ball et al. Theoretical issues in PDF determination and associated uncertainties. Phys.Lett., B723:330–339, 2013.

[52] S. Alekhin, J. Bluemlein, and S. Moch. The ABM parton distributions tuned to LHC data. Phys.Rev., D89:054028, 2014.

[53] S. Alekhin, S. Alioli, R. D. Ball, V. Bertone, J. Blumlein, et al. The PDF4LHC Working Group Interim Report. arXiv:1101.0536, 2011.

[54] J. H. Kuhn, M. Steinhauser, and C. Sturm. Heavy Quark Masses from Sum Rules in Four-Loop Approximation. Nucl.Phys., B778:192–215, 2007.

[55] E. Bagnaschi, R.V. Harlander, S. Liebler, H. Mantler, P. Slavich, et al. Towards precise predictions for Higgs-boson production in the MSSM. JHEP, 06:167, 2014.

[56] LHC Higgs Cross Section Working Group, S. Dittmaier, C. Mariotti, G. Passarino, and R. Tanaka (Eds.). Handbook of LHC Higgs Cross Sections: 1. Inclusive Observables. CERN-2011-002, 2011.

[57] P. Bechtle, T. Bringmann, K. Desch, H. Dreiner, M. Hamer, C. Hensel, M. Krämer, N. Nguyen, W. Porod, X. Prudent, B. Sarrazin, M. Uhlenbrock, P. Wienemann. Constrained Supersymmetry after two years of LHC data: a global view with Fittino. JHEP, 1206:098, 2012.

[58] W. Beenakker, R. Hopker, and M. Spira. PROSPINO: A Program for the production of supersymmetric particles in next-to-leading order QCD. arXiv:hep-ph/9611232, 1996.

[59] T. Plehn. `http://www.thphys.uni-heidelberg.de/~plehn/index.php?show=prospino&visible=tools`.

[60] J. M. Campbell, R. Frederix, F. Maltoni, and F. Tramontano. NLO predictions for t-channel production of single top and fourth generation quarks at hadron colliders. JHEP, 10:042, 2009.

[61] R. D. Ball, V. Bertone, F. Cerutti, L. Del Debbio, S. Forte, et al. Impact of Heavy Quark Masses on Parton Distributions and LHC Phenomenology. Nucl.Phys., B849:296–363, 2011.

[62] M. Botje, J. Butterworth, A. Cooper-Sarkar, A. de Roeck, J. Feltesse, et al. The PDF4LHC Working Group Interim Recommendations. arXiv:1101.0538, 2011.

[63] G.C. Branco, P.M. Ferreira, L. Lavoura, M.N. Rebelo, Marc Sher, et al. Theory and phenomenology of two-Higgs-doublet models. Phys.Rept., 516:1–102, 2012.

[64] LHC Higgs cross section working group. `https://twiki.cern.ch/twiki/bin/view/LHCPhysics/CrossSections`.